Adaptation of Kurganov-Tadmor's numerical scheme for applying in combination with the PISO method in numerical simulation of flows in a wide range of Mach numbers

M.Kraposhin, ISP RAS
S. Strizhak, HP
A. Bovtrikova, ISP RAS

Numerous problems of gas dynamics require modeling of turbulent compressible flows in a wide range of Mach numbers. The possibility of ensuring solution's monotonicity in discontinuities is one of the main criteria of quality estimation of the method during computational modeling of such flows. In resolving practical issues this is achieved by using such special schemes as discontinuity-disintegration scheme (approximate solution of the Riemann's problem), Kurganov-Tadmor's scheme (KT), [1-3], AUSM+ scheme [4-5] etc.

Implementations of these schemes in commercial packages as well as in OpenFOAM open source software package of different versions ([6], [7]) made a good showing while resolving problems of viscous and non-viscous liquid flows. The only disadvantage of its using is the medium's velocity limitation at the lower boundary of applicability range: the minimum Mach number must approach to the transonic conditions. Employing these models for viscous flow simulation with low Mach numbers (< 0.3) is impossible even with decreasing enough the time step to prevent the acoustic Courant criteria to be greater or equal to 1/2. Such limitations creates several impediments for studies of devices' aerodynamics in marginal conditions with the help of a single model – for example, while changing from the subsonic to the supersonic flow conditions.

At the same time there is a range of semi-implicit methods for solving subsonic problems that are successfully employed in industry for high Mach number flows — PISO, SIMPLE and their combinations ([8]). The inconvenience of these methods consists in occurrence of numerical oscillations in the regions of flow properties' discontinuities, that take place in high-speed flows — for example, Kurganov-Tadmore scheme and the PISO algorithm are compared in [9] .

The solution might be found in hybrid scheme's implementation, for which PISO/SIMPLE algorithms for implicit integration of the mass (1), momentum (2) and energy (3) conservation equations are employed in combination with corresponding schemes for the non-oscillating discretization of the convective terms.

$$\frac{\partial \rho}{\partial t} + \nabla \cdot \left(\rho \vec{U} \right) = 0 \qquad (1)$$

$$\frac{\partial \rho \vec{U}}{\partial t} + \nabla \cdot (\rho \vec{U} \vec{U}) = \nabla \cdot \Pi + \vec{F}_b \quad (2)$$

$$\frac{\partial \rho e}{\partial t} + \nabla \cdot (\rho \vec{U} e) = \nabla \cdot (\Pi \cdot \vec{U}) - \nabla \cdot \vec{q} \quad (3)$$

Where ρ - density, $\vec{U}$ — velocity of the medium, $\vec{F}_b$ — the main vector of mass forces Π , — the normal and viscous tension tensor, e — the total energy of the flow (the sum of kinetic and internal energies), — $\vec{q}$ heat flux. According to the Newtonian liquid approach the tension tensor is computed via the strain rate tensor and the pressure's field $\Pi = -pI + \mu\left(\nabla \vec{U} + (\nabla \vec{U})^T\right)$, where p — pressure, I — unitary matrix, — dyna μ mic viscosity. The Fourier's law is engaged to calculate the heat flux:, where $\vec{q} = -\lambda \nabla T$, T — medium's temperature, λ — heat conductivity. It is assumed that medium is a perfect gas, i. e. , $p = \rho \widetilde{R} T$ $\widetilde{R} = R/M$ - individual gas constant, R — universal gas constant, M — molar mass of the considered gas.

Attempts to develop such hybrid schemes have already been made, for example in [10] it is suggested to use AUSM + scheme together with the PISO algorithm. Despite the promising results presented in the article, the search of source code implementation of the proposed technique has failed. Moreover, in our opinion, the AUSM+ technique has the following disadvantages: 1) the complexity of implementation, and 2) the presence of adjustable coefficients — model constants.

Therefore, we decided to pay attention to Kurganov-Tadmor's scheme (or rather its Kurganov-Noelle-Petrova version, or abbreviated KNP) which on one hand is already explicitly implemented in OpenFOAM package and has been repeatedly tested, and on the other hand it is simple enough to be used as part of a hybrid scheme. Another important feature of this scheme is independence of approximating expressions for the fluxes of physical quantities from the characteristics of the studied system of equations. Thus, there is no need to use solution expansion on characteristics for calculation of flows. The limitation of Kurganov-Tadmor's scheme is the need to maintain the acoustic Courant number less than 1/2, which leads to understated time steps in the case of low-velocity medium. Furthermore, non-physical "circuital" time oscillations appear when solving subsonic tasks.

Our proposed hybrid scheme based on PISO and KT/KNP, on the one hand, meets the requirement on monotonicity, and on the other hand it would allow simulating flow in a wide range of Mach numbers 0 < M < 6. In this case, simulation in the range of low and very low Mach numbers (M < 0.5) would be possible with an acoustic Courant number far exceeding 1. The idea of the method consists in the introduction of a switcher which when approaching to subsonic speed range would switch approximate expressions for fluxes to a standard form used in PISO method:

$$\int_V \nabla \cdot \vec{U} \Psi \, dV = \int_S d\vec{S} \cdot (\vec{U} \Psi) = \sum_f \Psi_f (\vec{U}_f \cdot d\vec{S}_f) = \sum_f \Psi_f \varphi_f \quad (4)$$

Where Ψ — some transferable value, f index — No. of a face of a cell , $d\vec{S}_f$ —

product of vector of a face normal on its area. Values with f index are interpolated on a surface mesh from volume mesh. To compare the designations of KT/KNP scheme, proposed in [1-3] with standard designations, used in the finite volume method, see Fig. 1. P point indicates the center of some control volume for which balances of mass, momentum and energy are considered. In one-dimensional case, point P of this volume has X_j coordinate. Expressions for flows are written for the right boundary of this volume, with the normal directed along the X axis from P point to N point, location of face center — $X_{j+1/2}$, location of the a neighboring volume center N - X_{j+1}.

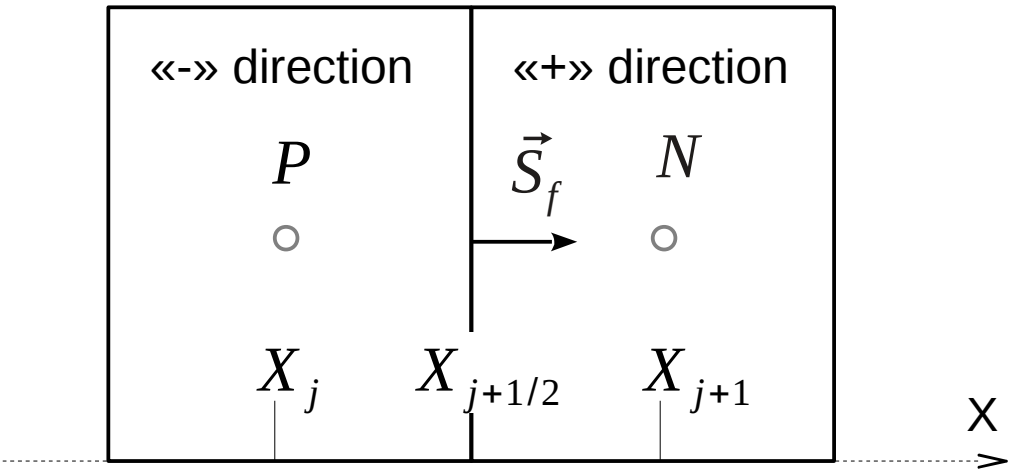

Fig. 1. Comparison of finite volume computing molecule in case of unstructured meshes (OpenFOAM) and structured meshes (KT/KNP)

In this case, according to KT/KNP [1-3] scheme, Ψ value flux through the face can be represented as a weighted sum of fluxes in positive and negative directions. In particular, the advective fluxes include not only macroscopic velocity of the medium, but also acoustic speed of disturbances propagation:

$$\Psi(X_{j+1/2})\varphi(X_{j+1/2}) = \frac{a^+_{j+1/2} f(\Psi^-_{j+1/2}) - a^-_{j+1/2} f(\Psi^+_{j+1/2})}{a^+_{j+1/2} - a^-_{j+1/2}} + \frac{a^+_{j+1/2} a^-_{j+1/2}}{a^+_{j+1/2} - a^-_{j+1/2}} \left(\Psi^+_{j+1/2} - \Psi^-_{j+1/} \right) \qquad (5)$$

To switch to the designation system used in the finite volume method we introduce the following designation:

$$a_f^{max} = a^+_{j+1/2},\ a_f^{min} = -a^-_{j+1/2},\ \alpha_f^P = \frac{a_f^{max}}{a_f^{max} + a_f^{min}},\ \alpha_f^N = \frac{a_f^{min}}{a_f^{min} + a_f^{max}}$$

$$\Psi_f^P = \Psi^-_{j+1/2},\ \Psi_f^N = \Psi^+_{j+1/2},\ \varphi_f^P = f(\Psi^-_{j+1/2}),\ \varphi_f^N = f(\Psi^+_{j+1/2}),\ \omega_f = \alpha_f^P a_f^{min}$$

Then, the expression for the calculation of convective flux of ψ value through the face takes the form of [6]:

$$\Psi_f \varphi_f = \alpha_f^P \varphi_f^P \Psi_f^P + \alpha_f^N \varphi_f^N \Psi_f^N + \omega_f \left(\Psi_f^P - \Psi_f^N \right) \qquad (6)$$

or after transposition of terms

$$\Psi_f \varphi_f = \Psi_f^P \left(\alpha_f^P \varphi_f^P + \alpha_f^P a_f^{min}\right) + \Psi_f^N \left(\alpha^N \varphi^N - \alpha_f^P a_f^{min}\right) \quad (7)$$

Here, the superscript indicates the cell, which value is used for interpolation on the face *f*, if *P* then the cell is used, with respect to which the normal is external, if *N* then the cell is used, with respect to which the normal is internal.

To calculate the coefficients α_f^P , α_f^N we use volume fluxes a_f^{max} a_f^{min} and , relative to local sound speed in the medium

$$\begin{aligned} a_f^{max} &= max\left(c_f^P |\vec{S}_f| + \varphi_f^P, c_f^N |\vec{S}_f| + \varphi_f^N\right) \\ a_f^{min} &= -min\left(-c_f^P |\vec{S}_f| + \varphi_f^P, -c_f^N |\vec{S}_f| + \varphi_f^N\right) \\ c_f^P &= \sqrt{\gamma_f^P \widetilde{R} T_f^P} \\ c_f^N &= \sqrt{\gamma_f^N \widetilde{R} T_f^N} \end{aligned} \quad (8)$$

Where $\gamma = Cp/Cv$ — adiabatic number of gas

To calculate the values o Ψ_f^P f and o Ψ_f^N n the face we use interpolation schemes of the second order with a limiter. Generally, we use symmetric TVD schemes — vanLeer, Minmod, vanAlbad, etc. as a limiter.

As already mentioned, KT/KNP scheme implemented in OpenFOAM is explicit, which makes it unsuitable for the study of flows with small numbers M < 0.5. In order to achieve the possibility of simulating flows in this range, including those with small time steps, we have proposed a hybrid scheme, which allows combining properties of PISO/SIMPLE and KT/KNP algorithms using a switch function. The idea of a hybrid scheme is as follows:

1) Formulate mass fluxes in the form (7) according to the KT/KNP schemes

2) Introduce some mixing function which allows “switching” between incompressible and compressible flux formulations.

3) Write the equation of conservation of mass and momentum and energy in semidiscrete form suitable for derivation of the pressure equation.

4) Apply PISO/SIMPLE method to discretize equations in which the convective terms are approximated by means of “switcher” function and KT/KNP scheme (7).

The use of this approach not only greatly simplifies the implementation of schemes in OpenFOAM, but also allows accounting turbulence with built-in library functions. To mix subsonic and supersonic formulations, write the mass fluxes using the mixing function κ_f :

$$\begin{aligned} \Phi_f^P &= \kappa_f \rho_f^P \left(\alpha_f^P \varphi_f^P + \alpha_f^P a_f^{min}\right) \\ \Phi_f^N &= \rho_f^N \left(\alpha_f^N \varphi_f^N - \alpha_f^P a_f^{min}\right) + (1 - \kappa_f) \rho_f^P \left(\alpha_f^P \varphi_f^P + \alpha_f^P a_f^{min}\right) \end{aligned} \quad (9)$$

When using the KT scheme instead of KNP, the form of terms will change, but the concept

will remain. With the increasing influence of compressibility s κ_f witch shall strive for 1, and then Φ_f^N and Φ_f^P - fluxes degenerate into mass fluxes, calculated based on KT/KNP scheme. Instead, when approaching κ_f to 0, flux strive Φ_f^N s for for the flux formulation in an incompressible approach, and Φ_f^P flux strives for 0.

Based on the above description of the proposed hybrid scheme (which can be interpreted as a requirement), we can propose the following form of this κ_f function :

$$\kappa_f = min(M_f / CFL, 1) \tag{10}$$

To get the final equation for the pressure, write the integral analog of momentum conservation equation (2) in the discrete form:

$$A\vec{U} = \frac{1}{V}\vec{H} - \nabla p \tag{11}$$

Where A — diagonal coefficients of the matrix, $\vec{H}$ — total contribution of the off-diagonal matrix coefficients, and V — volumes of cells.

The continuity equation (1) in the discrete form with convective fluxes substituted from (9):

$$\frac{\delta\rho}{\delta t} + \frac{1}{V}\sum_f \left(\Phi_f^N + \Phi_f^P\right) = \frac{\delta\rho}{\delta t} + \frac{1}{V}\sum_f \left(\rho_f^N\left(\alpha_f^N \varphi_f^N - \alpha_f^P a_f^{min}\right) + \rho_f^P\left(\alpha_f^P \varphi_f^P + \alpha_f^P a_f^{min}\right)\right) = 0 \tag{12}$$

Where $\delta/\delta t$ — operator of discrete partial differentiation with respect to time.

φ_f^N and φ_f^P fluxes are calculated by the interpolated velocity obtained in accordance with semidiscrete expression (11) in the control volume centers N and P, as it is done in the standard method of PISO or SIMPLE

$$\begin{aligned} \varphi_f^N &= \left(\frac{1}{V}\frac{\vec{H}}{A}\right)_{f,N} \cdot \vec{S}_f - \left(\frac{\nabla p}{A}\right)_{f,N} \cdot \vec{S}_f \\ \varphi_f^P &= \left(\frac{1}{V}\frac{\vec{H}}{A}\right)_{f,P} \cdot \vec{S}_f - \left(\frac{\nabla p}{A}\right)_{f,P} \cdot \vec{S}_f \end{aligned} \tag{13}$$

Substituting the expression for convective flows (13) and the perfect gas equation of state in discrete continuity equation, we obtain the equation for the pressure generated taking into account KT/KNP scheme:

$$\frac{\delta \psi p}{\delta t} +$$
$$\frac{1}{V}\sum_f \left[(\psi p)_f^N \left(\alpha_f^N \left[\left(\frac{1}{V}\frac{\vec{H}}{A} \right)_{f,N} \cdot \vec{S}_f - \left(\frac{\nabla p}{A} \right)_{f,N} \cdot \vec{S}_f \right] - \alpha_f^P a_f^{min} \right) \right] + \tag{14}$$
$$\frac{1}{V}\sum_f \left[(\psi p)_f^P \left(\alpha_f^P \left[\left(\frac{1}{V}\frac{\vec{H}}{A} \right)_{f,P} \cdot \vec{S}_f - \left(\frac{\nabla p}{A} \right)_{f,P} \cdot \vec{S}_f \right] + \alpha_f^P a_f^{min} \right) \right] = 0$$

Here $\psi = 1/(\tilde{R}T)$ — gas compressibility.

This equation is non-linear with respect to the pressure due to:

1) Presence of pressure as a coefficient in diffusion terms.

2) Dependency of $\alpha_f^P a_f^{min}$ and $\alpha_f^P a_f^{min}$ terms on unknown φ_f^N and φ_f^P fluxes, which themselves depend on pressure..

Thus, to solve it we need linearization. The practice of testing of the proposed scheme on various models has showed that the use of the values of these coefficients from the previous step with the technique of internal iterations is sufficient to achieve the required accuracy of the results and to ensure the mesh convergence.

Approximation of convective transport of other variables (velocity and total energy) is performed by means of fluxes (9), which are obtained by solving the equation for the pressure (14). As for the rest, integration algorithm of system of equations of fluid corresponds to well-known methods of operators splitting class — PISO, SIMPLE, etc.

The described hybrid scheme has been implemented by means of the finite volume library OpenFOAM 2.3.0 as an application – **pisoCentralFoam** “solver”, and tested for a wide range of Ma and Re numbers.

1. Wave propagation in channel of constant area (SODA's problem).

Shock wave propagation in a cylindrical channel was investigated. The wave is generated by the expansion of compressed air of high pressure and temperature to the region of low pressure and temperature. The scheme of the problem is presented in Fig. 2. Gas in both right and left zones is the air. This one-dimensional problem has its analytical solution [11]. At the initial time point the regions of different pressures are separated with a diaphragm. After the diaphragm's rupture a compressive wave begins its propagation in the low pressure direction, the same for an exhaustion

wave in the high pressure direction. Depending on the left and right pressure ratio the gas stream can be subsonic or supersonic. The both cases were considered during testing of pisoCentralFoam solver.

Table 1. Initial conditions

Region	Subsonic flow		Supersonic flow	
	Pressure, Pa	Temperature, K	Pressure, Pa	Temperature, K
Left part of the diaphragm	P_4=6,897*10^4	T_4=288,89	P_4=6,897*10^4	T_4=288,89
Right part of the diaphragm	P_1=5,897*10^4	T_1=288,89	P_1=6,897*10^3	T_1=231,11

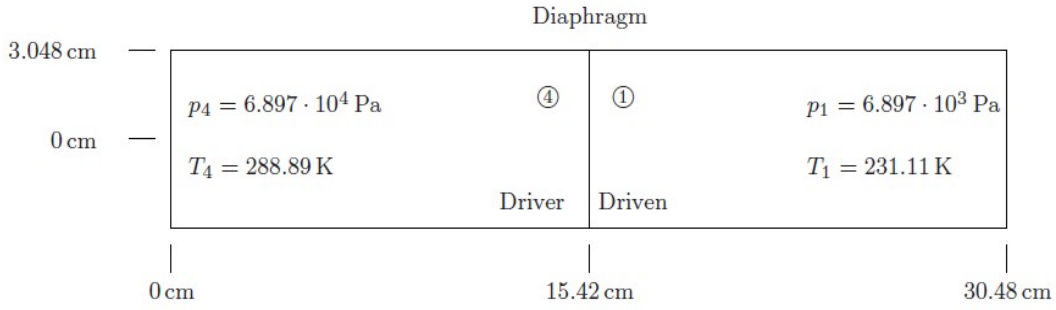

Fig. 2. Computational domain for the case of wave propagation in a channel

The pisoCentralFoam solver's testing was realized for 1D (100 cells), 2D (1000 cells), 2D axially symmetrical (1000 cells) and 3D (30000 cells) approximations to detect the influence of problem's dimension on the result. Computational domains with mesh lines for 2D and 3D cases are presented in Fig. 3.

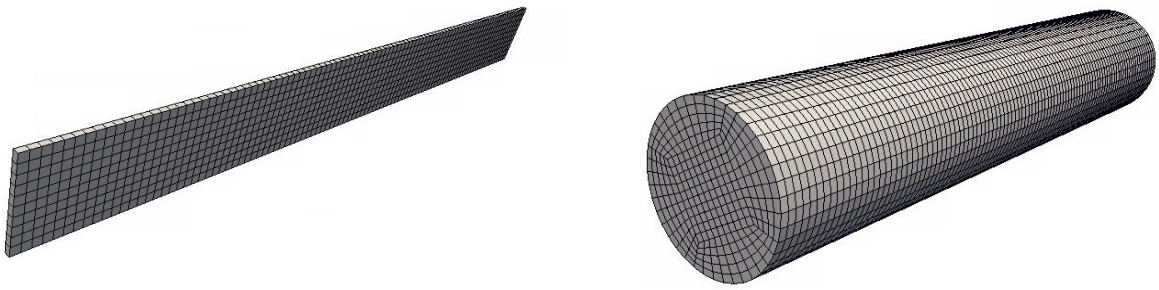

a) b)

Fig. 3. Variants of computational mesh (a — 2D, b-3D) for SODA's problem

The computation was conducted up to the moment t=0.00025s. The results show that distribution of the pressure in cross-section is uniform in 2D in 3D cases, and the solution of the problem does not depend on dimension. Comparison of one-dimensional case results with the

analytical solution is given in Fig. 4 and Fig. 5. These figures show, that the numerical solution, obtained with developed model is in good agreement with analytical solution and does not oscillate.

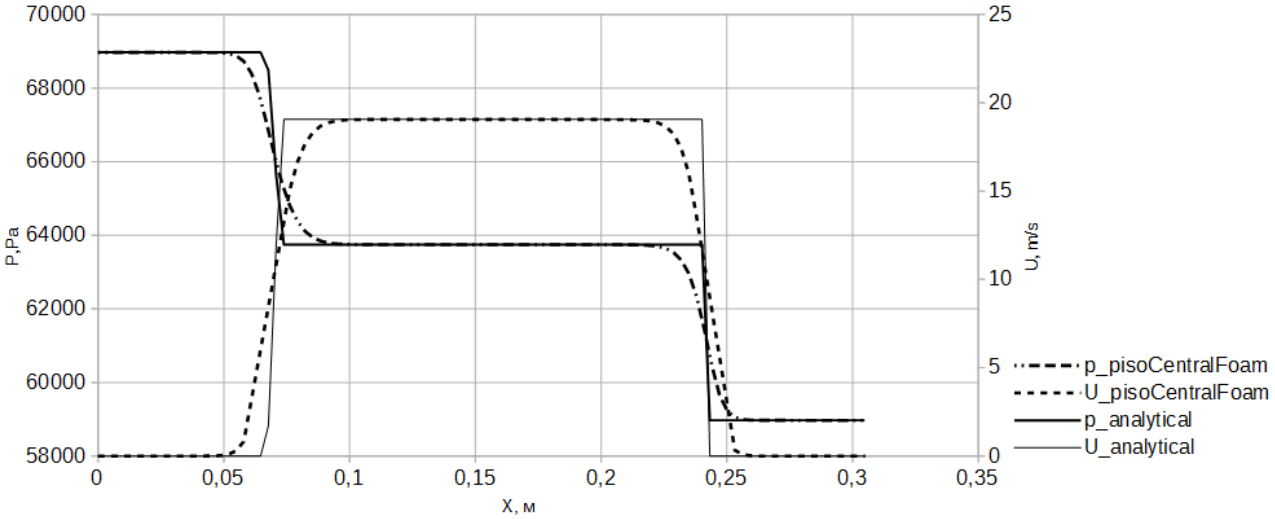

Fig. 4. Comparison of the calculation and analytical pressure distribution along the tube axis for the subsonic case.

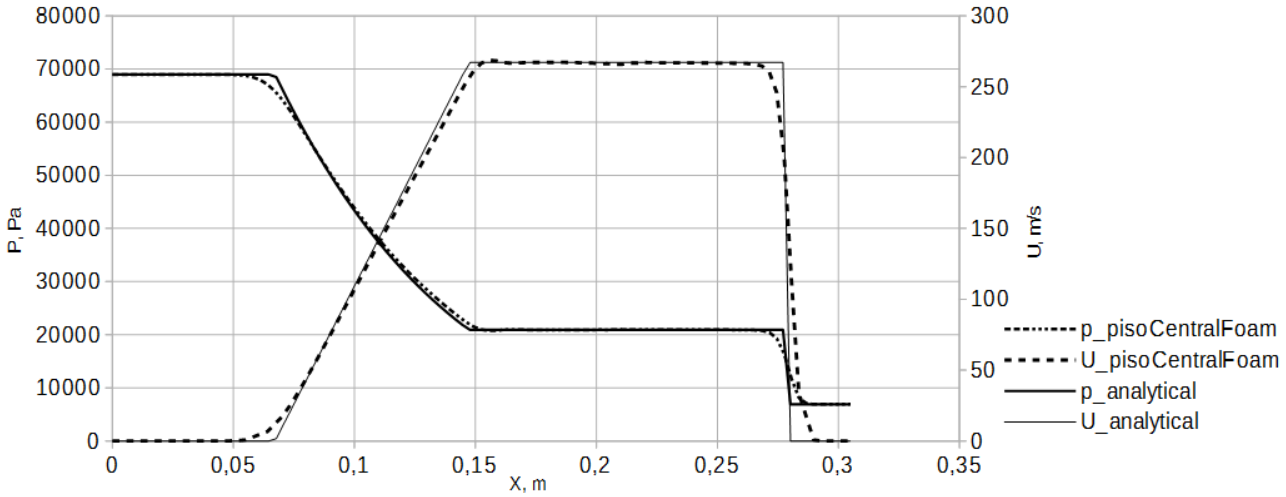

Fig. 5. Comparison of the calculation and analytical pressure distribution along the tube axis for the supersonic case.

2. Flow over a two-dimensional wedge.

Supersonic flow over a two-dimensional wedge was examined in this case (Fig. 6). The work [12] was employed as the initial materials. The Mach number of the incident flow M=2.5. The actuating medium is dry air, its molar mass – 28.96 g/mol, specific gas constant – 287.05 J/kg/K. The hypothesis of possibility of actuating medium simulation by the way of an ideal gas was assumed. The pressure and the temperature of the incident flow are 101350 Pa and 288.9 K correspondingly.

Isobar heat capacity was assumed to be equal to 1004 J/kg/K, heat capacity ratio is equal to

1.4. Speed of sound in the medium – $\sqrt{(\gamma RT)}$ = 340.736 m/s. Inlet velocity $U = M \cdot a$ = 851.84 m/s. Dynamic viscosity was supposed to be 18.4 μPa-s and the Prandtl number Pr = 1.

As it is well known, this problem has an analytical solution within the theoretical framework of oblique shock wave (see [12]). Thus, the object of this simulation was to obtain convergence of computational results to the analytical solution. The Mach number was considered as a convergence estimator. It changes unevenly while passing the shock. For this purpose, a range of samples of parameters of the flow was taken at a distance of 0.05 m away along the Y-axis direction from the solid surface.

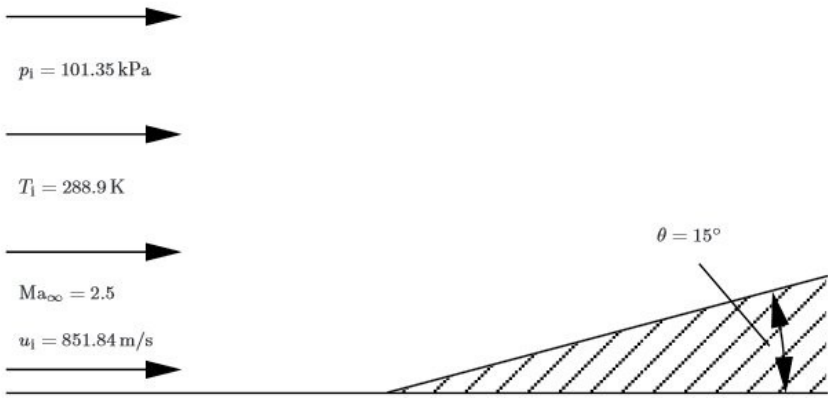

Fig. 6. Initial conditions of the oblique shock case.

A two-block two-dimensional mesh was constructed (see Fig. 7). The first block was a rectangle 0.1522x0.3048 m^2, the second one (above the wedge) – a right trapezium with the height of 0.3048 m, equal to the bottom base, and with the side face, inclined at 15 degrees from the X-axis. To verify the convergence of the scheme, the simulation was conducted on three meshes with different precision parameters. The initial decomposition of the blocks: 75x50 cells (the first block – 25x50; the second block – 50x50). To construct a finer or a rougher mesh the number of cells per block was scaled up or down 1.5 times.

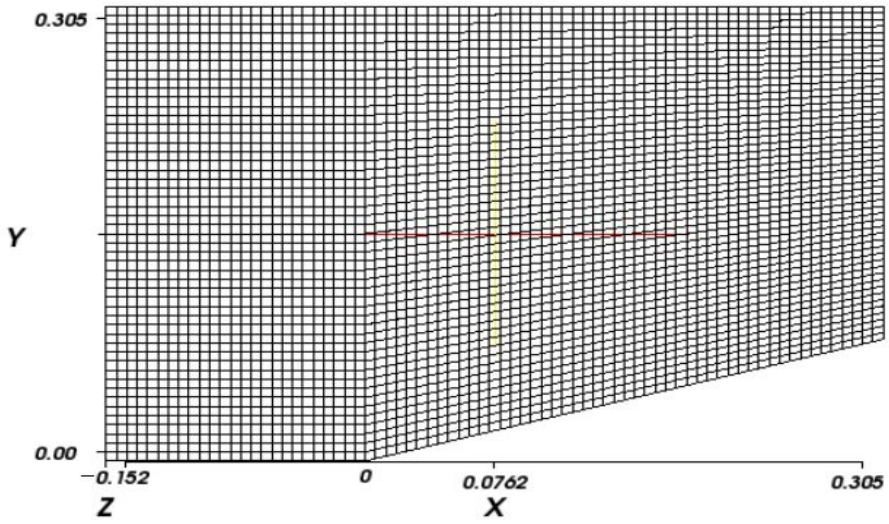

Fig. 7. Computational domain for the oblique shock case

Moreover, the influence of the order of time-discretization scheme on the convergence was studied. Euler implicit schemes of the first and the second order were investigated. Finally, the influence of Courant number limitation on the convergence ratio was observed. Pressure contours, showing position of shock are presented in Fig. 8.

Fig. 8. The image of the stream obtained with the simulation.

The calculation allowed to do the following conclusions:

•Usage of second order schemes for time discretization brings numerical solution closer to theoretical curve (fig. 9). But also it can lead to growth of oscillations.

•A stricter Courant number limitation increases the convergence ratio.

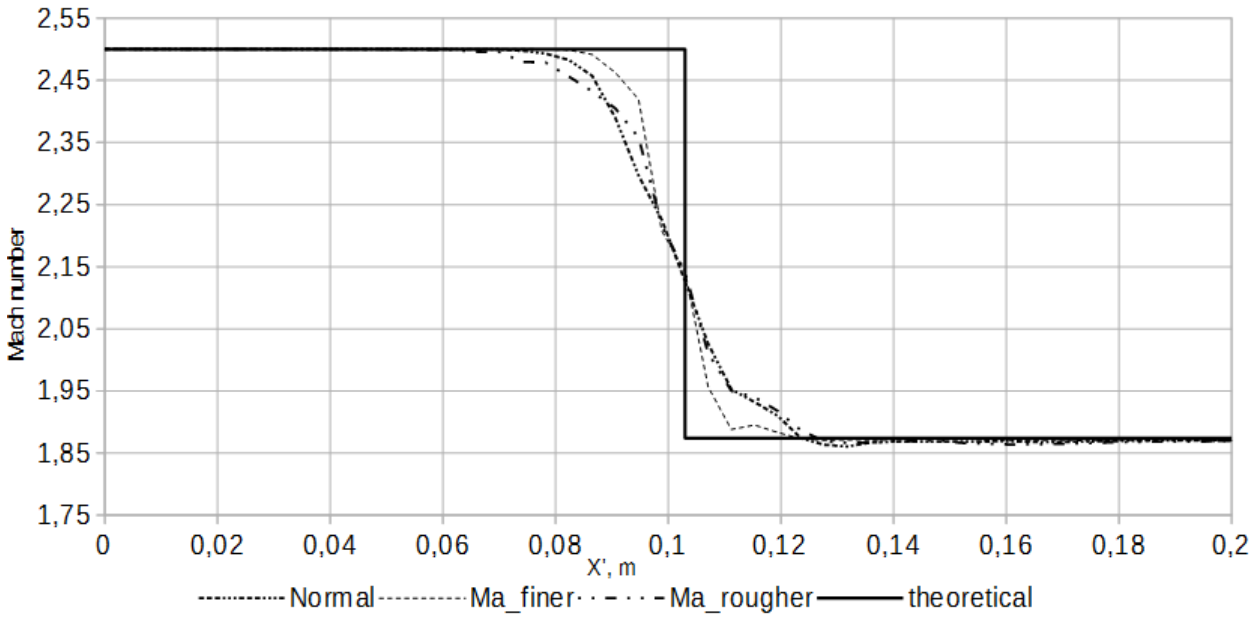

Fig. 9. Mesh convergence and comparison of numerical solution with theoretical for oblique shock case

3. Backward facing step.

For the third test case the classical problem from the theory of detached flow – two-dimensional flow over the backward-facing step – was studied. The picture of the flow is presented in figure 10. The flow expands while passing through the edge and forms the fan of waves of exhaustion. An obstacle in the form of horizontal surface determines the viscous flow separation. The reattachment leads to λ-shaped shock wave's formation.

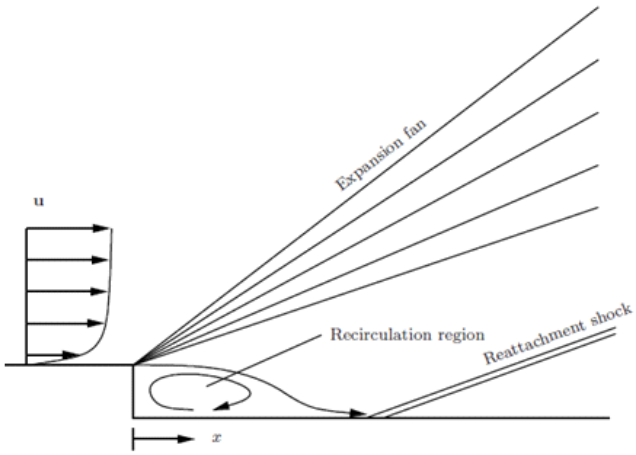

Fig. 10. Qualitative picture of the supersonic flow over backward step

Information from [13] was used as initial data. Mach number of the incident flow M=2.5. The actuating medium is dry air, its molar mass – 28.96 g/mol, specific gas constant – 2.544 MJ/kg/K. k- ω SST turbulence model was used. The turbulence parameters' assignment on inlet was performed with following dependencies: $k=3/2*(\bar{U}\ I)^2$, where $\bar{U}$ - is the average velocity, and I –

turbulence intensity, that assumed to be 5%; $\omega = \varepsilon/(k \cdot C_\mu)$, where the turbulence kinetic energy $\varepsilon = C_\mu^{3/4} \cdot k^{3/2}/l$, $l = 0{,}07L$, where L-characteristic dimension, and the coefficient $C\mu$=0.09.

Static pressure of the incident flow is 13316.6 Pa, the stagnation pressure is 227527 and the stagnation temperature is 344.44K.

Isobar heat capacity was assumed equal to 1005 J/kg/K, the heat capacity ratio γ=1.4. The speed of sound in the medium – $\sqrt{(\gamma R T)}$ = 248 m/s. Inlet velocity U = M * a = 620 m/s. Dynamic viscosity μ=18.27 μPa*s. Prandtl number Pr = 0.7.

The step's height is 0.01125 m, the distance from the step to the inlet is 0.1016 m, to the outlet – 0.3048 m, to the upper limit of the computational domain – 0.1475 m. The Reynolds number changes in the range from $7*10^3$ to $5*10^6$.

The mesh was constructed with 3 rectangular blocks. The first block sided with the step and counted 240x40 cells, the second one was located above the step (104x112 cells) and the third one closed the computational domain (240x112 cells).

For all the solid walls a no-slip boundary condition was assigned, k and ω were approximated with wall functions.

The results were compared to the experimental data from [14], and with computational data from PARC,WIND and ANSYS Fluid Dynamics codes. The computation was stopped after 0.06 s, when the flow became steady.

Comparison between pressure distribution obtained in this work and experimental and numerical data from other authors behind the step is shown in Fig. 11. Pressure is normalized with the static inlet pressure, and the coordinate in inches is measured from the step.

As we can see, pisoCentralFoam performs better with reference experimental and numerical data from [13], ANSYS Fluid Dynamics Guide. At the same time the curve, obtained with developed model, is slightly different from the data in the report [14] and from numerical results of WIND and PARC codes [15]. The pressure in the stagnation region is over-predicted relatively to these sources. We need to mention that the original reference experimental pressure distribution from [13] hasn't been found in report [14].

Result of conducted mesh convergence survey is presented in Fig. 12. It is seen from this Fig. that developed scheme is 2^{nd} order in space, and numerical solution tends to an accurate one after refining mesh with factor 4 in each direction in the region of separation.

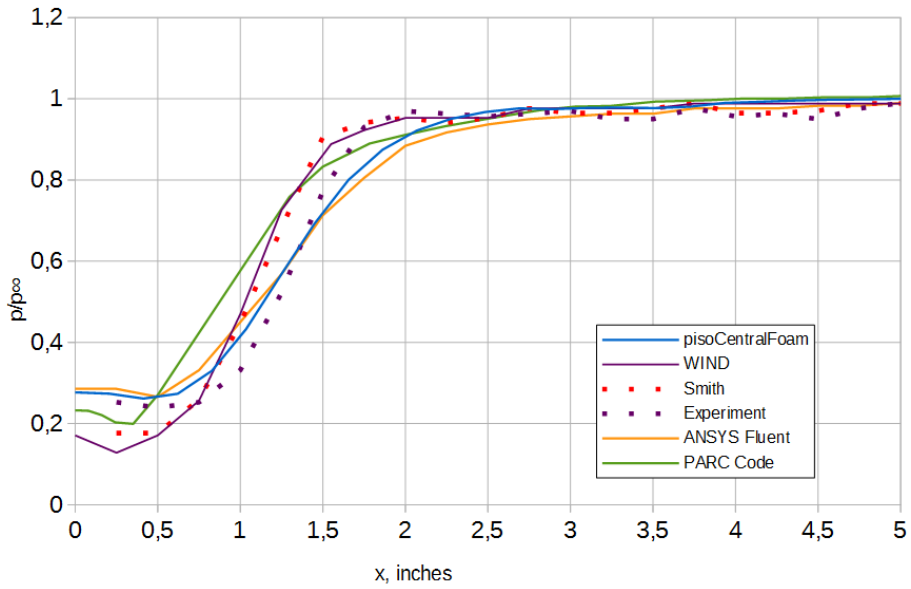

Fig. 11. Comparison of pressure distribution

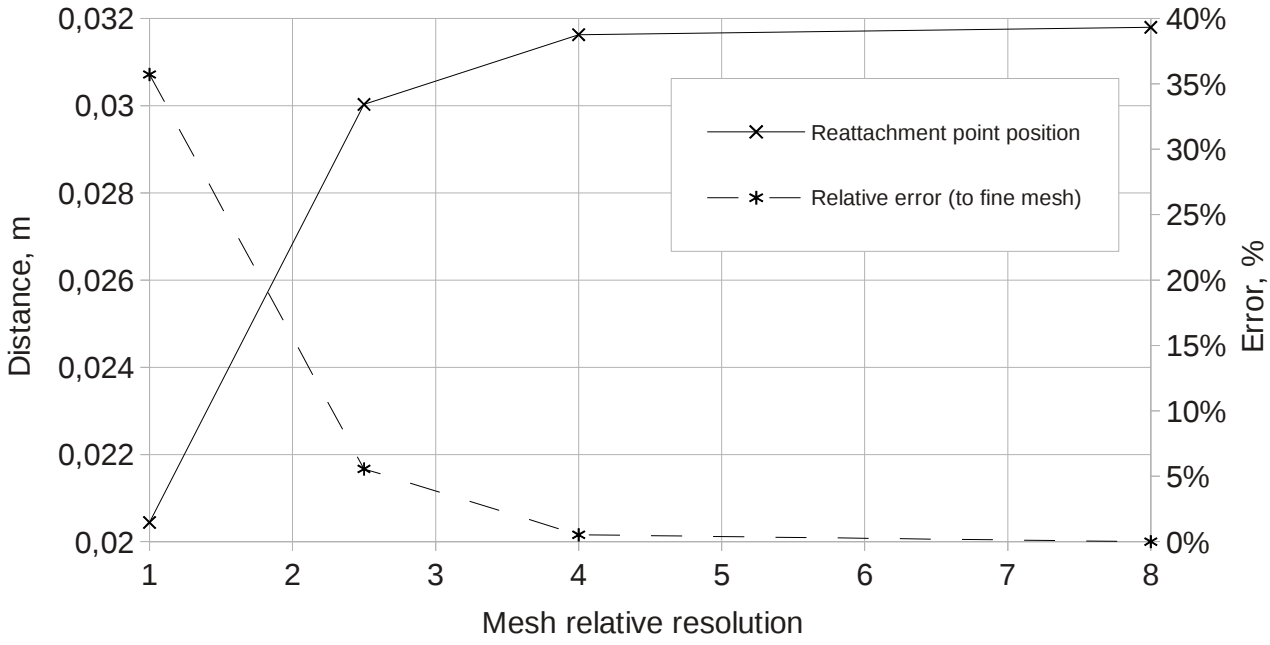

Fig. 12. Mesh convergence of the developed numerical scheme for the case of backward step

In order to qualitatively estimate correctness of resolution of supersonic flow spatial characteristics in the presence of shock we made comparison with experimental and numerical data. Fig. 13 shows flow structure, obtained with developed model and its comparison with experimental position of shock from [14] and numerical position of shock, obtained in PARC code [15]. As it can be seen from picture, our prediction of shock position both in good agreement with side numerical results and experimental data.

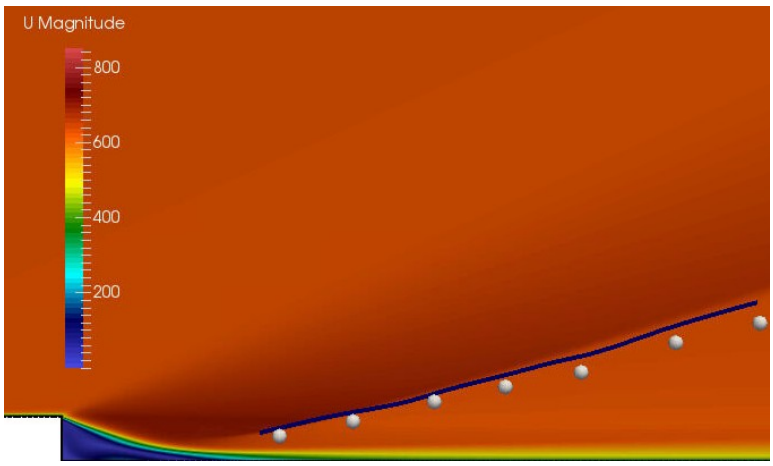

Fig. 13. Comparison of the reattachment shock location. Experimental position of shock marked with gray points, numerical position of shock, obtained with code PARC[15] shown with blue line

4. Flow in a supersonic nozzle with a normal shock in the divergent region.

The problem of a flow over the simplest supersonic nozzle was considered. The nozzle geometry was modeled with a combination of two truncated cones. The initial data correspond to the calculation case from [13]. The results were compared to the analytical solution based on the laws of isotropic flow of an ideal gas and the theory of normal shock [16], as well as to the results of simulation in ANSYS Fluid Dynamics.

The layout of the nozzle and the steady flow structure are represented in figure 14. The ratio of inlet and outlet cross-sections to the throat cross-section is equal to 3, the nozzle length was 2m (for simpler manipulation with the reduced coordinate of the normal shock).

Boundary conditions were defined with the inlet and outlet pressures, 300 and 175 kPa correspondingly. The slip condition on the walls was chosen. The flow was simulated as the non-viscous.

As far as the existing analytical solution is legible only for the one-dimensional approach (identical parameters through the nozzle's cross-section), a one-dimensional mesh was constructed (one cell in Y, Z directions; X-axis coincides with the nozzle's symmetry axis). The total number of cells in X- direction was 100.

Thus, the problem's statement was approximated at most to the problem's wording, corresponding to the analytical solution.

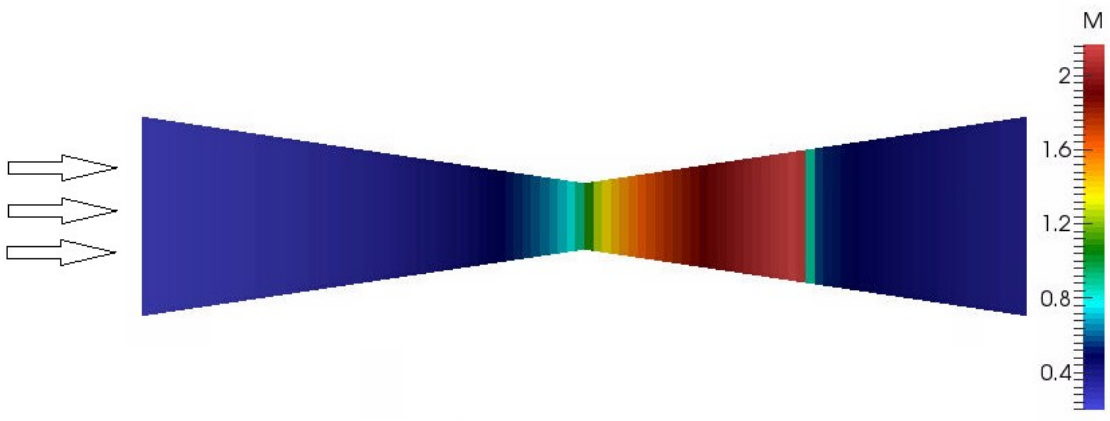

Fig. 14. Steady flow over the nozzle.

As it is seen on the figure 15, the analytical and computational Much number distributions practically coincide, except some divergence in the shock area, which could be explained with the diffusion of the scheme. The error value is less than 6 %.

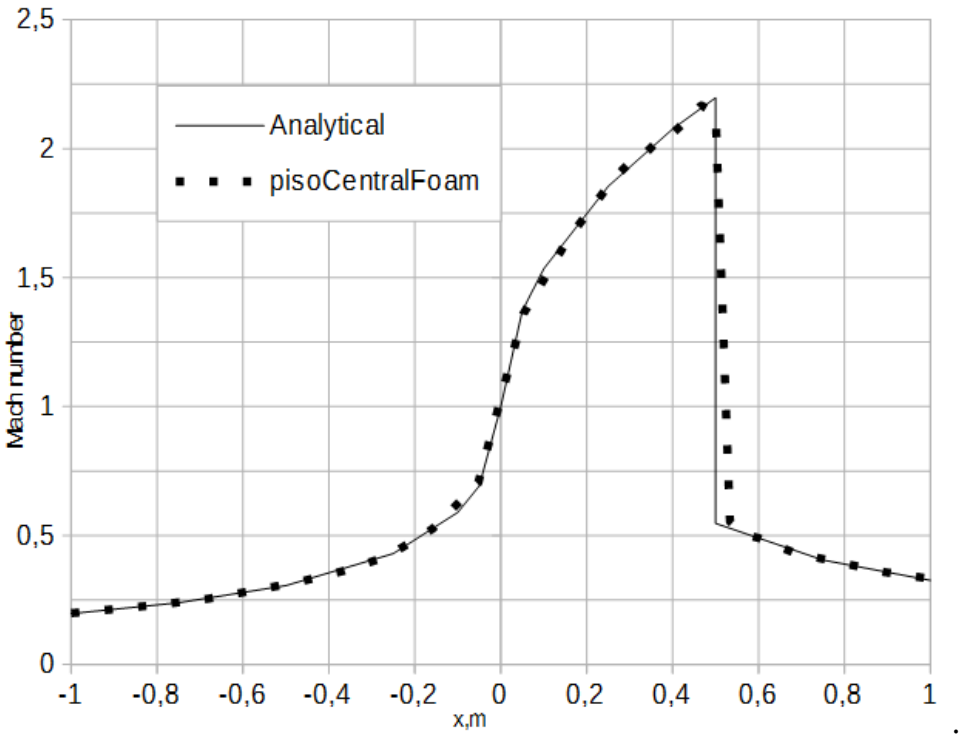

Fig 15.Comparison of Mach number's distribution along the nozzle's length.

5. Forward-facing step problem with supersonic flow

The supersonic flow of ideal inviscid gas is considered in the wind tunnel with a sharp narrowing (Fig.16). The wind tunnel is 1 unit length high and 3 units long. The step is 0.2 units high and is located 0.6 units from the inlet on the left. The tunnel is assumed to be infinitely wide in the direction orthogonal to the computational plane. The parameters of splittings are specified in table 3. The velocity, pressure and temperature are distributed uniformly at initial time point on all space of the channel. The boundary conditions are:

- On a ledge (it is shaded) the sticking condition is defined for flow velocity (zero velocity), the condition of adiabatic wall for temperature (zero gradient), impermeability condition for pressure (zero gradient);

- On the top and bottom horizontal boundaries the slip condition is defined for flow velocity, the condition of adiabatic wall for temperature, impermeability condition for pressure.

- On the inlet of domain (left vertical boundary) – fixed value for velocity (3 m/s), pressure (1 Pa), temperature (1 K)

- On the outlet of domain (right vertical boundary) – zero gradient for velocity, pressure, and temperature

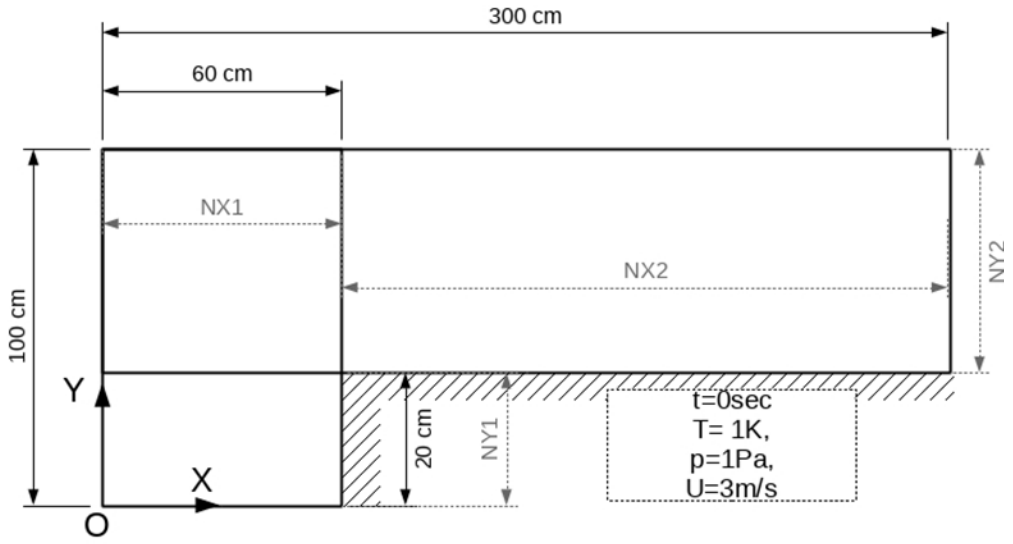

Fig. 16 Scheme of simulation domain and splitting into blocks

The case uses a gas with γ =1.4 and is initialized with p=1,T=1 and Mach 3. For simplicity, we set specific gas constant R=0.714, so that the speed of sound c=1 and the flow velocity u=(3,0,0) corresponds directly to the Mach number. The molar weight is set to 11640.3 g/mol, adiabatic thermal capacity 2.5 J/ (kgK), Prandtl number Pr=1, dynamic viscosity = 0 kg/м/c. The solution to this problem evolves from t=0 to t=4 s.

Space discretization parameters are provided in Table 3. The calculation was performed until T=4sec time. We compared the position of λ-shaped shock wave's “leg” and the presence/absence of

Kelvin-Helmholtz instability observed in many studies during reproduction of the case. Given the correct discretization is present at T=4sec moment of time, the position of λ-shaped shock wave's “leg” shall fall within the leading ledge (X=60cm).

This case was used to test the scalability of the model and investigation of the mesh convergence with respect to time and space. The results of the mesh convergence are provided only for medium, refined and very fine meshes. Parameters of coarse mesh are for reference only.

Table 3. The parameters of splitting for simulation domain

№	Segment	Number of splittings, coarse grid	Number of splittings, moderate grid	Number of splittings, fine grid	Number of splittings, very fine grid
1	NX1	96	192	384	768
2	NX2	384	768	1536	3072
3	NY1	32	64	128	256
4	NY2	128	256	512	1024
			Size of computational mesh		
		60 thous.	250 thous.	1 mln.	4 mln.

Based on the calculations it becomes clear that regardless of the degree of refining of the estimated mesh the position of λ-shaped shock wave's corresponds to the position of the step (see Fig. 17). In this case, when using the first-order scheme with respect to time, Kelvin-Helmholtz instability starts to appear only on the finest mesh (4 million cells), while the use of the second-order approximation scheme with respect to time allows reproducing this effect on a more coarse mesh as well (1 million cells) — see Fig. 18. Investigation of solver's scalability (Fig. 19) has showed satisfactory acceleration on 1 million cells mesh and superlinear acceleration for 4 million cells mesh. Superlinear acceleration possibly occurs due to inability to accommodate all the data of the numerical model (4 million cells) in the cache of the processor in single-processor calculation mode, which has led to overvalued relative acceleration .

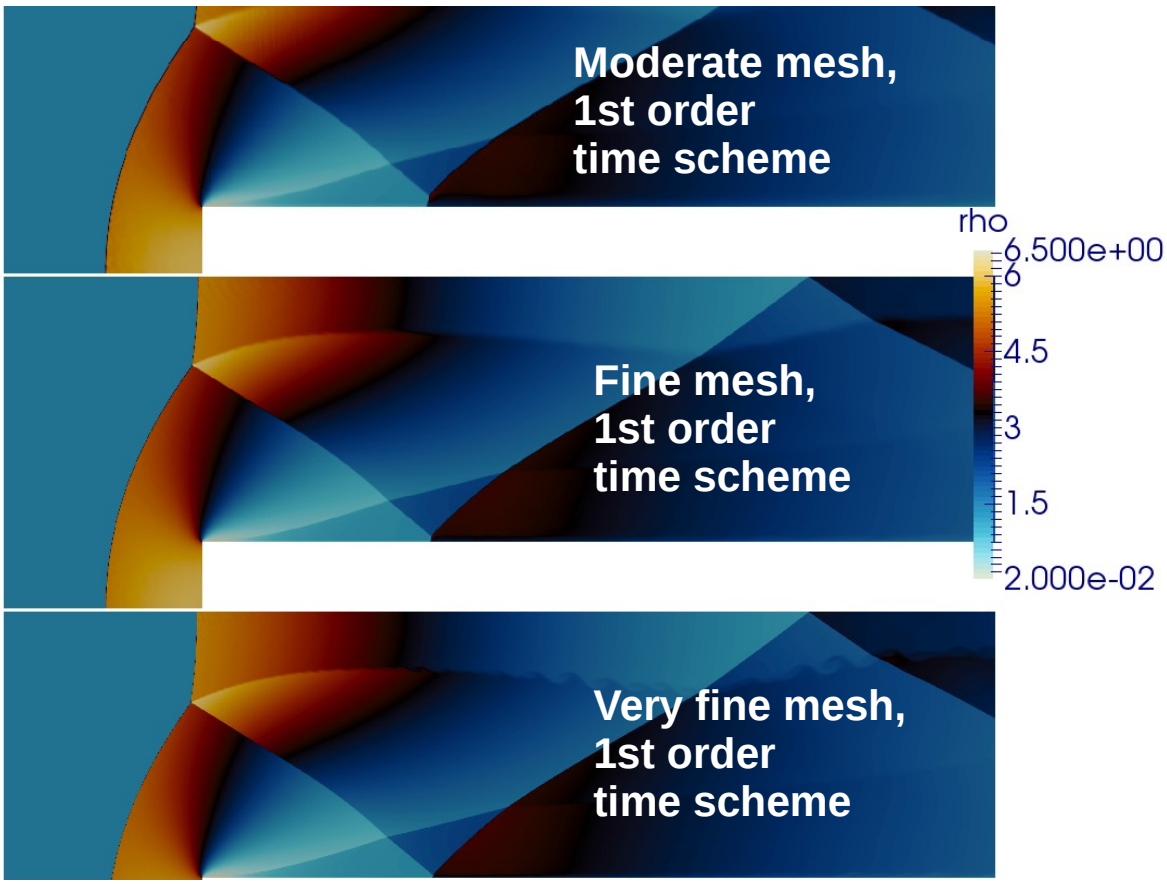

Figure 17. Comparison of flow patterns (density field) for “medium” mesh, fine mesh and very fine mesh at T=4sec moment of time. The first-order of approximation with respect to time and the second order of approximation with respect to space.

Figure 18. Comparison of flow patterns (density) for the case calculated with the first order of approximation with respect to time on the finest mesh, and for the case calculated with the second order of approximation with respect to time on a coarser mesh

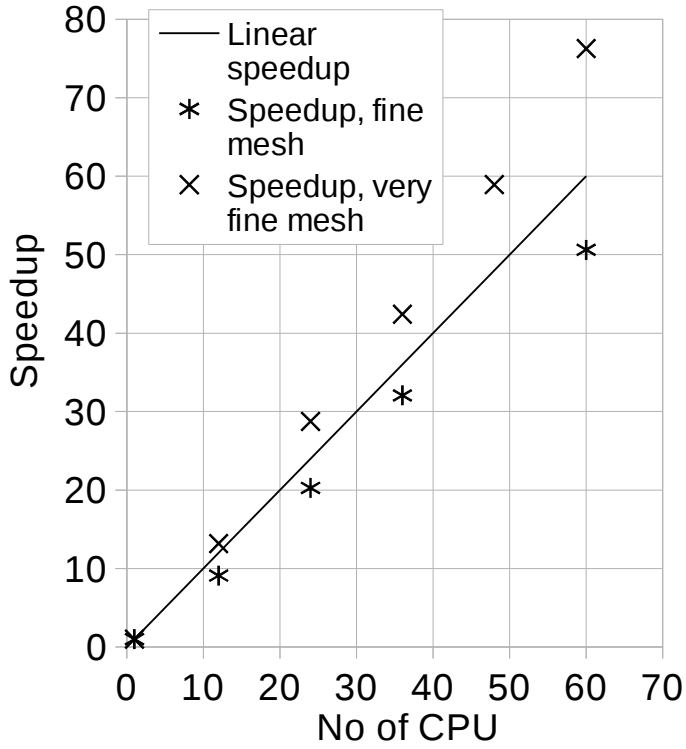

Figure 19. Comparison of scalability of the developed solver for 1 million cells mesh and 4 million cells mesh.

6.**Subsonic laminar viscous flow in the channel of round cross section**

By means of this calculation case we check the validity of reproduction of diffusion terms in momentum conservation equation (strain tensor) at low Mach numbers. As for this case the analytical solution is known, it is possible to assess the accurate quantity of error between the exact and approximate solutions. For the formulation of the task, it is assumed that the number Re=200, viscosity is calculated from the physical data defined in the formulation of initial and boundary conditions.

It is assumed that the boundary conditions correspond to normal conditions: inlet velocity U_{in}=0,68369м/с; outlet pressure p_{out}=101325Pa; temperature — 25 ^{0}C; gas — air. The velocity profile at the inlet to the study area even.

According to the parameters of the medium and the target: Prandtl number Pr=0.73, dynamic viscosity $\mu=1.85\cdot10^{-5}$ Pa/sec., heat capacity Cp=1007 J/kg/K, molar mass M=28.96g/mol.

The computational domain is a sector of a cylindrical channel with a length substantially greater than the diameter of the channel for laminar profile at the outlet.

To get a specified value of Re criterion, diameter of the computational domain is selected to be 4.6mm, length — 161mm. To obtain a uniform mesh, the computational domain is divided into

23 segments radially, and 1610 segments lengthwise.

The results of comparison of analytical solutions for laminar profile at the outlet of the computational domain and numerical solution, obtained by means of this model are shown in Figure 15. The Mach number amounted to 0.002. The calculation was conducted with a time step of 30-40 mus, which corresponds to the acoustic Courant number of ~ 1300.

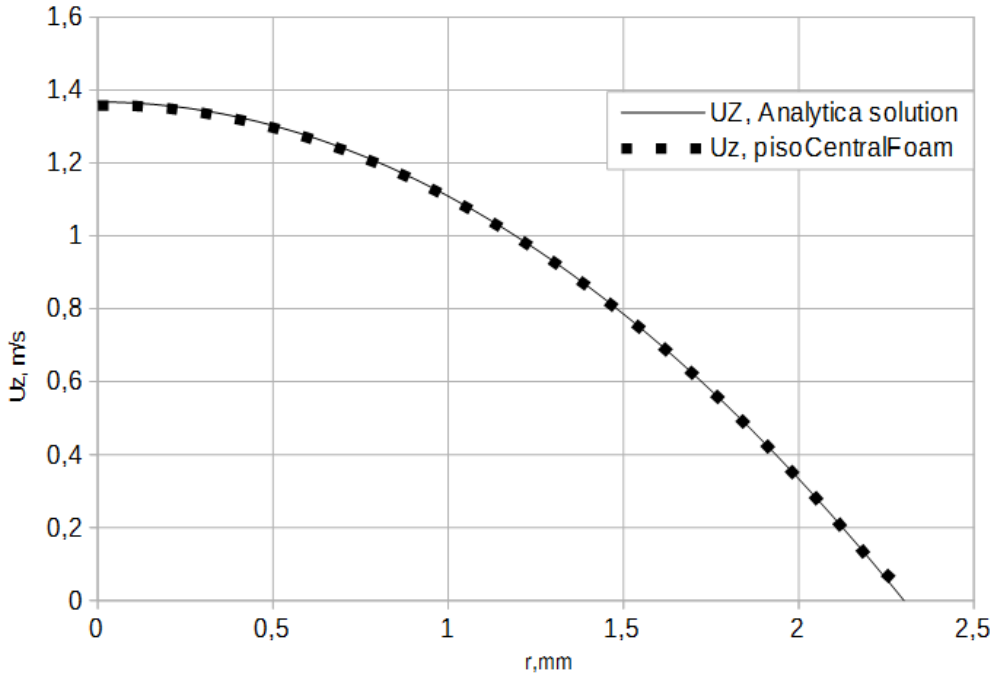

Fig. 20. The comparison of analytical and calculated distributions of Uz(r) in the channel with round section.

7. Subsonic flow around single cylinder

Using this test, we study the suitability of the implemented model for simulation of subsonic flows for such a well-known case, as the flow around bluff bodies. The study is carried out in two cases — laminar flow and turbulent flow. The study of the last case is particularly important in the perspective of the goal of the use of already existing in the OpenFOAM library turbulence models without its change.

7.1. Laminar flow around cylinder

The results of calculations of paper [17] are taken as a basis. The comparison is carried out for two values of Mach number – less than 0.1 and 0.2 which correspond to two maximum permissible cases – "deep" subsonic (completely incompressible flow) and compressible flow. The number of Re is 100. Pressure and temperature conditions are similar to normal – 101325 Pa and 300K, respectively, a working environment – air, molar weight – 28.9 g/mol get out close to normal.

Thus, environment density under these conditions will be equal to the following: 1.17404 kg/m3, the isobaric thermal capacity is accepted equal to 1004 J/ (kgK), therefore, γ is equal to 1.4 The speed of sound of the environment – sqrt (γ/psi) = 347.6 m/s, dynamic viscosity of the environment is taken as equal to 18.5 muPa-s, the Prandtl number Pr = 0.73. The diameter of the cylinder is determined according to the velocity at the inlet and Re number.

By assuming U = 10 m/s, which corresponds to Mach number 0.029, we obtain the value of the diameter of the cylinder 0.000157m (0.157mm). By assuming U = 100 m/s, which corresponds to Mach number 0.29, we obtain the value of the diameter of the cylinder 0.0157mm.

Cd drag coefficient acted as criterion for checking the correctness of results of calculation. Table 4 provides comparison of the coefficients of resistance received by means of pisoCentralFoam solver against other numerical and pilot studies given in [17].

It is also worth mentioning that the frequency of vortex shedding and oscillation amplitude coefficient of drag of the cylinder is also in good coincidence with the known data.

Table 4. The value of Cd

	pisoCentralFoam	ACL 2008-4	Sharman 05	Mene-01	Kang (2003)	Ding 07
Cd	1.37	1.365	1.33	1.37	1.33	1.356

7.2. Subsonic turbulent flow around a cylinder**.**

The flow around a single cylinder is simulated (Fig. 21), and the results are compared with the results of the study [18]. In addition to comparison with experiment, we performed the comparison with the calculation of incompressible and compressible subsonic models available in OpenFOAM.

The turbulent flow around single cylinder is modeled, results are compared with paper [18]. A working environment — air, conditions — similar to normal (pressure of 101325 Pa and temperature 300K), density — 1.18 kg/m3, kinematic viscosity — 1.5*10-5 sq.m/s, speed of sound is about 330 m/s. Velocity of flow during the experiments was accepted ~ 10 m/s, i.e. the number of the Mach was less than 0.1 — this is “deeply“ subsonic flow. During experiments values of force of front resistance of X and lift force Y were measured and on their values the coefficient of front resistance of Cd and coefficient of lift force Cl paid off.

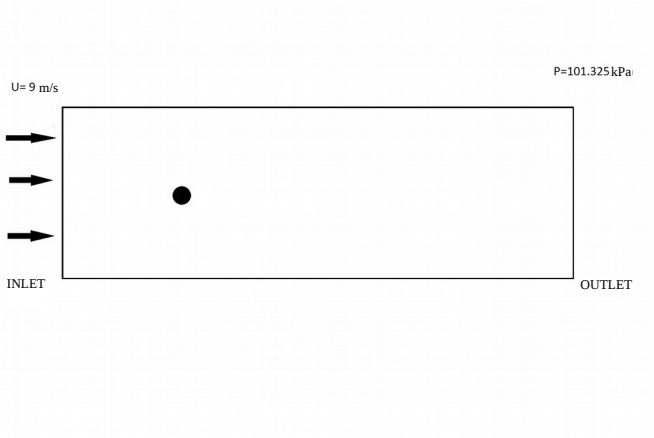

Fig. 21. Simulation domain

The simulation was carried out for a cylinder flow case with a diameter of 12.22 cm at Reynolds's (Re) number equal to 7.3*10e5 (velocity of flow U = 9 m/s) from here. Intensity of kinetic energy of turbulence in experiment changed by installation on an entrance of lattices with a different form and the size of cells and made in the considered case 0.7% - Fig. 22. Cd value in experiment was 1.22.

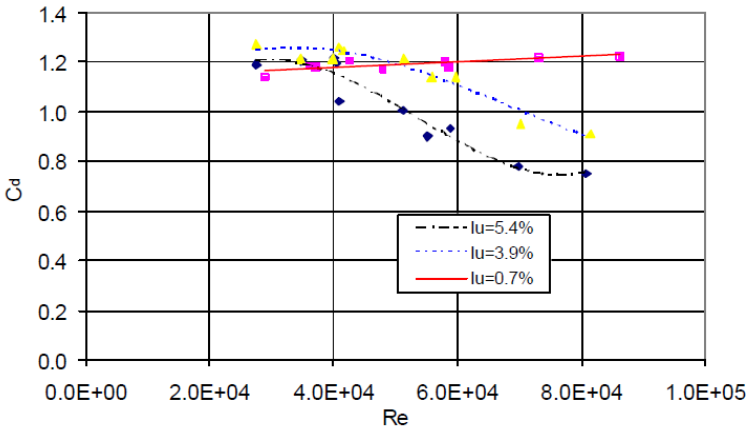

Fig. 22. Experimental data for Cd with single cylinder

On the first stage of modeling for debugging of model, calculations were carried out in incompressible approach. Calculation was conducted before the set flow mode. The turbulence was considered with use of the k-omega SST model. Options of different grids with the low permission near a cylinder surface (y + ~ 100, calculations were carried out with use of wall functions), and grids with high resolution near a cylinder surface were considered (y + ~ 1, the wall functions aren't used). By the received results for further research the second option of a grid was chosen (see Fig. 23).

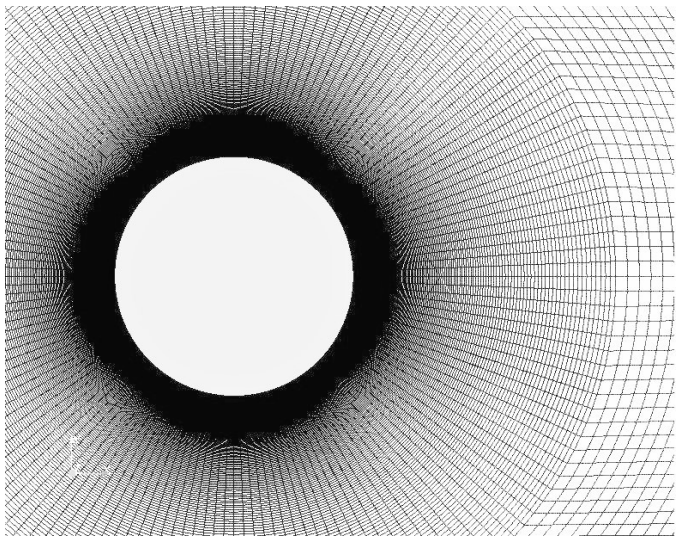

Fig. 23. The grid for single cylinder.

On boundaries of simulation domain the following boundary conditions were set:

1) inlet – fixed value for velocity, k, omega and temperature for compressible cases; zero gradient for pressure;

2) on outlet – fixed value for pressure, zero gradient for other variables

3) on cylinder wall: slip condition for velocity, wall functions were used for k and omega;

4) on top and bottom boundaries – slip condition;

In simulation domain the temperature and velocity were set equal to temperature and speed on the inlet, pressure — equal to the pressure at the outlet.

At approach of the set flow mode in simulation domain, the periodic separation of vortices from a surface of the cylinder and the development of a vortex path (a so-called path of Karman) was watched behind the cylinder.

Owing to a separation of vortices the value of coefficient of front resistance Cd fluctuates in time. Therefore, as results the value average on time *Cd* on time interval after approach of the set flow mode was considered.

The further calculations in incompressible approach by means of a solver of pisoCentralFoam using the numerical scheme of Kurganov-Tadmor were carried out. The calculations were carried out on a grid with y + ~ 0.8, wall functions weren't used. Results of comparison of experiment, calculation in an incompressible solver of pimpleFoam, the standard compressible rhoPimpleFoam solver, and also in the solver of pisoCentralFoam investigated in this work are given in table 5.

Table 5. The results of Cd simulation

№	The description	The name of solver	The value of C_d
1	Experiment	-	1,22
2	Calculation with incompressible solver (y^+~0.8, I_{inlet}=0%)	pimpleFoam	1,15
3	Calculation on fine grid with compressible solver	pisoCentralFoam	1,07
4	Calculation on fine grid with compressible solver	rhoPimpleFoam	1,12

Conclusion

We have proposed and implemented a hybrid semi-implicit model of viscous perfect gas flow with the field of applicability in a wide range of Mach numbers – from deep incompressible flow (Ma <0.1) to supersonic flow (M> 3). The developed model is based on the adaptation of the explicit Kurganov-Tadmor scheme (and its KNP modification) for the use as part of the PISO operators splitting method.

The advantage of the scheme is the combination of the best features of each of these approaches in one model:

- Simple implementation within the finite volume method for unstructured meshes and high degree of parallelism (KT/KNP and PISO).
- Monotonicity of solution (KT/KNP).
- Flexible applicability of different approximation schemes with respect to time and space (PISO).
- The possibility of sustainable numerical simulation of subsonic flows with a time step which corresponds to Courant number >> 1 (PISO).
- Automatic switching between the subsonic, transonic and supersonic schemes.
- Support of existing OpenFOAM functional library (or other finite volume package).

The model was tested in compressible and incompressible approximation for one-dimensional, two-dimensional and three-dimensional flows in a wide range of Reynolds and Mach numbers. The obtained results show a good degree of coincidence with the analytical functions and experimental data. Mesh convergence of the method is demonstrated with respect to space and time. It is shown that the scheme achieves the 2nd order of approximation.

We have shown the possibilities of the use of scheme in parallel mode. Testing was performed on 1 million cells meshes and 4 million cells meshes, and the number of cores from 1 to 60. We have shown the possibility of nearly linear acceleration even with a small ratio of the number of cells on the compute core.

Bibliography

[1] Alexander Kurganov, Eitan Tadmor «New High-Resolution Central Schemes for Nonlinear Conservation Laws and Convection–Diffusion Equations» // Journal of Computational Physics 160, 241–282 (2000), doi:10.1006/jcph.2000.6459

[2] Kurganov A, Noelle S, Petrova G. «Semi-discrete central-upwind schemes for hyperbolic conservation laws and Hamilton–Jacobi equations» // SIAM Journal on Scientific Computing 2001; 23:707–740

[3] Kurganov A, Petrova G. «Central-upwind schemes on triangular grids for hyperbolic systems of conservation laws» // Numerical Methods for Partial Differential Equations 2005; 21:536–552

[4] M.S. Liou, C.J. Steffen Jr. «A new flux splitting scheme» // J. Comput. Phys., 107 (1) (1993), pp. 23–39

[5] M.S. Liou «A sequel to AUSM: AUSM^{+}» // J. Comput. Phys., 129 (2) (1996), pp. 364–382

[6] Christopher J. Greenshields, Henry G. Weller, Luca Gasparini and Jason M. Reese «Implementation of semi-discrete, non-staggered central schemes in a colocated, polyhedral, finite volume framework, for high-speed viscous flows» // Int. J. Numer. Meth. Fluids 2010; 63:1–21, DOI: 10.1002/fld.2069

[7] Shen Chuna, Sun Fengxianb, Xia Xinlina «Analysis on capabilities of density-based solvers within OpenFOAM to distinguish aerothermal variables in diffusion boundary layer» // Chinese Journal of Aeronautics, Volume 26, Issue 6, December 2013, Pages 1370–1379, http://dx.doi.org/10.1016/j.cja.2013.10.003

[8] J.H. Ferziger, M. Peric «Computational Methods for Fluid Dynamics» // 3d Edition, Springer, 2002

[9] Luis F. Gutiérrez Marcanton, José P. Tamagno, Sergio A. Elaskar «HIGH SPEED FLOW SIMULATION USING OPENFOAM» // Mecánica Computacional Vol XXXI, páges. 2939-2959 (artículo completo), Salta, Argentina, 13-16 Noviembre 2012

[10] C. M. Xisto, J. C. Páscoa, P. J. Oliveira and D. A. Nicolini «A hybrid pressure–density-based algorithm for the Euler equations at all Mach number regimes» // Int. J. Numer. Meth. Fluids (2011), DOI: 10.1002/fld.2722

[11] Anderson, Jr, John D. «Modern Compressible Flow: With Historical Perspective» // Third edn. New York: McGraw-Hill, 2003

[12] Benjamin Wuthrich, «Simulation and validation of compressible flow in nozzle geometries and validation of OpenFOAM for this application» // Master Thesis 2007.

[13] ANSYS Fluid Dynamics Verification Manual, Release 15.0, 2013.

[14] Smith, Howard E. «The Flow Field and Heat Transfer Downstream of a Rearward Facing Step in Supersonic Flow» // Technical report ARL 67-0056. Aerospace Research Laboratories, Ohio, 1967 (Mar.)

[15] G. D. Garrard, W.J. Phares. «Calibration of the PARC Program for Propulsion-Type flows», 1991

[16] F. M.White. «Fluid Mechanics» // 3rd Edition. McGraw-Hill Book Co., New York, NY. 518531. 1994.

[17] Chunlei Liang. «High-order accurate simulation of low-Mach laminar flow past two side-by-side cylinders with Spectral Difference method» // Report ACL 2008-4 Aerospace Computing Laboratory, Aeronautics and Astronautics, Stanford University, May 2008

[18] Xianzhi Liu, «Wind loads on multiple cylinders arranged in tandem with effects of turbulence and surface roughness» // Master thesis, Department of Civil and Environmental Engineering, Louisiana State University, 2003.